

FIT: a Fast and Accurate Framework for Solving Medical Inquiring and Diagnosing Tasks

Weijie He*,¹ Xiaohao Mao*,¹ Chao Ma,² José Miguel Hernández-Lobato,^{2,3} Ting Chen¹

¹ Department of Computer Science & Institute of Artificial Intelligence & BRNist, Tsinghua University, Beijing, China 100084

² Department of Engineering, University of Cambridge

³ Microsoft Research Cambridge

{hbj19, mxh19}@mails.tsinghua.edu.cn, {cm905, jmh233}@cam.ac.uk, tingchen@tsinghua.edu.cn

Abstract

Automatic self-diagnosis provides low-cost and accessible healthcare via an agent that queries the patient and makes predictions about possible diseases. From a machine learning perspective, symptom-based self-diagnosis can be viewed as a sequential feature selection and classification problem. Reinforcement learning methods have shown good performance in this task but often suffer from large search spaces and costly training. To address these problems, we propose a competitive framework, called FIT, which uses an information-theoretic reward to determine what data to collect next. FIT improves over previous information-based approaches by using a multimodal variational autoencoder (MVAE) model and a two-step sampling strategy for disease prediction. Furthermore, we propose novel methods to substantially reduce the computational cost of FIT to a level that is acceptable for practical online self-diagnosis. Our results in two simulated datasets show that FIT can effectively deal with large search space problems, outperforming existing baselines. Moreover, using two medical datasets, we show that FIT is a competitive alternative in real-world settings.

Introduction

In healthcare, self-diagnosis through online services is a promising approach for reducing costs and still maintaining wide accessibility. However, online search-based services for self-diagnosis often return irrelevant information and sometimes absurd results. With the explosive development of mobile internet and big data techniques, the need for online self-diagnosis in the healthcare domain has increased. A growing number of adults first attempt to self-diagnose their illness or diseases through online search services instead of walking into a hospital. According to a 2012 survey (Semigran et al. 2015), 35% of U.S. adults regularly use the internet to self-diagnose.

As described by Ledley and Lusted (1959), a disease diagnosis process includes three sequential steps: (i) a patient presents an initial symptom, (ii) a doctor inquires a patient with a series of reasonable questions, (iii) a final diagnosis for a disease is given by the doctor. In the case of online self-diagnosis, the above process is referred to as symptom

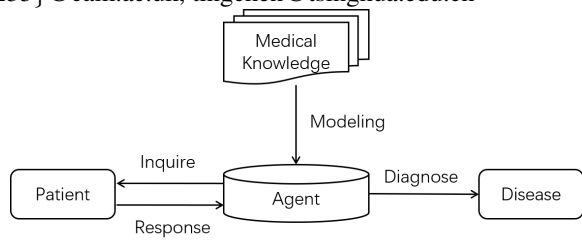


Figure 1: The logic components of symptom checking. (Tang et al. 2016)

checking and it is an agent who implements inquiry and diagnosis instead of the doctor. Figure 1 presents the logical components of symptom checking.

From the healthcare perspective, high disease-prediction accuracy is the primary aim of symptom checking. High accuracy requires a long list of possible symptoms. For example, most existing questionnaire systems acquire a large number of symptom values from the patient through exhaustive questions (Shim, Hwang, and Yang 2018; Lewenberg et al. 2017). This is inefficient and time consuming for both the patient and the expert. Therefore, the other design goal of symptom checking is efficiency; in other words, the number of inquiries should be as low as possible.

From the machine learning perspective, symptom checking can be viewed as a sequential feature selection and classification problem. Reinforcement learning (RL) methods have shown good performance in this task (Tang et al. 2016; Kao, Tang, and Chang 2018; Peng et al. 2018; Xia et al. 2020). However, they often suffer from large search spaces and struggle during training. An alternative is given by EDDI, a framework for instance-based active feature acquisition (Ma et al. 2019), which chooses the next feature to observe by maximizing a defined information reward over all features. EDDI uses a Partial VAE to handle data with missing values. Such a model can deal with the situation where an agent just knows part of the information from patients while inquiring. Although promising, the EDDI framework is limited by its high computational cost when the number of symptoms is very high.

To address these problems, we propose FIT, a competitive

*The first two authors contributed equally to this paper.

framework to automate symptom-based self-diagnosis based on EDDI. The contributions of this paper are:

- A novel and practical framework for symptom checking. FIT has two main advantages over previous RL methods. First, FIT can make predictions at any step of the self-diagnosis process and achieve high performance, while the previous RL methods only return the disease prediction at the end of inquiry. Second, FIT is more suitable for real-life diagnosis since it can handle large disease spaces better than RL baselines, which typically struggle in those settings.
- Improvements on model. Instead of VAEs (Kingma and Welling 2013), we use a multi-modal variational autoencoder (MVAE) (Wu and Goodman) as a probabilistic model for dealing with partially observed data. The main difference of MVAE over the original VAE (Kingma and Welling 2013) is that it uses a product of experts (PoE) encoder. Furthermore, to make better predictions, we adopt a two-step sampling strategy. Both MVAE and our two-step sampling strategy significantly improve the accuracy of disease diagnosis.
- Significant speed-up of computations. We accelerate the inquiry steps so that they take less than one second on average, making our framework practical in real-life settings. At any inquiry step, we first ignore irrelevant symptoms that are unlikely to co-occur with the ones currently observed and second, when computing the information reward, we ignore the contribution of symptoms whenever they are predicted to be not present given the current context. Both modifications can reduce the time cost of our self-diagnosis framework by three orders of magnitude.

Background

Problem Formulation

In this paper, we consider the following feature acquisition problem: given a data point \mathbf{x} , we are interested in predicting the target variables of interest $\mathbf{x}_\phi \subset \mathbf{x}_U$ given corresponding observed features \mathbf{x}_O ($\mathbf{x}_\phi \cap \mathbf{x}_O = \emptyset$), where \mathbf{x}_O is the set of observed variables, and \mathbf{x}_U are the unobserved ones. More specifically, we consider which variable $\mathbf{x}_i \in \mathbf{x}_{U \setminus \phi}$ to observe next, so that our belief regarding \mathbf{x}_ϕ can be optimally improved.

Variational AutoEncoder (VAE)

A variational autoencoder (VAE) (Kingma and Welling 2013) defines a generative model of the form $p(\mathbf{x}, \mathbf{z}) = \prod_i p_\theta(\mathbf{x}_i | \mathbf{z}) p(\mathbf{z})$ in which the data \mathbf{x} is generated from latent variables \mathbf{z} , $p(\mathbf{z})$ is a prior, e.g. spherical Gaussian. $p_\theta(\mathbf{x} | \mathbf{z})$ is given by a neural network decoder with parameters θ , which specify a simple likelihood, e.g. Bernoulli. A VAE uses another neural network with parameters Φ as an encoder to produce a variational approximation of the posterior, that is, $q_\Phi(\mathbf{z} | \mathbf{x})$. A VAE is trained by maximizing an evidence lower bound (ELBO):

$$E_{q_\Phi(\mathbf{z} | \mathbf{x})} [\log p_\theta(\mathbf{x} | \mathbf{z})] - \beta \cdot D_{\text{KL}}[q_\Phi(\mathbf{z} | \mathbf{x}) \| p(\mathbf{z})], \quad (1)$$

where β is the weight to balance the two terms in the expression. The ELBO is usually optimized by stochastic gradient descent using the reparameterization trick (Kingma and Welling 2013).

EDDI Framework Formulation

EDDI is a recently proposed solution (Ma et al. 2019) that is designed to solve the formulated feature acquisition problem efficiently using a VAE. EDDI chooses the next feature \mathbf{x}_i to observe by maximizing over i the information reward

$$R(i, \mathbf{x}_O) = \mathbf{E}_{\mathbf{x}_i \sim p(\mathbf{x}_i | \mathbf{x}_O)} D_{\text{KL}}[p(\mathbf{x}_\phi | \mathbf{x}_i, \mathbf{x}_O) \| p(\mathbf{x}_\phi | \mathbf{x}_O)], \quad (2)$$

where D_{KL} is the Kullback-Leibler divergence between two distributions. The conditionals $p(\mathbf{x}_i | \mathbf{x}_O)$, $p(\mathbf{x}_\phi | \mathbf{x}_O, \mathbf{x}_i)$, and $p(\mathbf{x}_\phi | \mathbf{x}_O)$ are described by a VAE. Unfortunately, estimating the values of these quantities in Eqn. 2 is too expensive in practice. To avoid this problem, Ma et al. (2019) show that Eqn. 2 can be estimated efficiently by using VAE encoding distributions:

$$\hat{R}(i, \mathbf{x}_O) = \mathbf{E}_{\mathbf{x}_i \sim \hat{p}(\mathbf{x}_i | \mathbf{x}_O)} D_{\text{KL}}[q(\mathbf{z} | \mathbf{x}_i, \mathbf{x}_O) \| q(\mathbf{z} | \mathbf{x}_O)] - \mathbf{E}_{\mathbf{x}_\phi, \mathbf{x}_i \sim \hat{p}(\mathbf{x}_\phi, \mathbf{x}_i | \mathbf{x}_O)} D_{\text{KL}}[q(\mathbf{z} | \mathbf{x}_\phi, \mathbf{x}_i, \mathbf{x}_O) \| q(\mathbf{z} | \mathbf{x}_\phi, \mathbf{x}_O)], \quad (3)$$

where $q(\cdot)$ is the encoder function of the underlying VAE model. The encoder is parameterized by a permutation invariant set function (detailed in the next section), so that it is able to produce a Gaussian approximation of the posterior of \mathbf{z} conditioned on any set of observed variables. The first term of Eqn. 3 quantifies how much information \mathbf{x}_i provides about \mathbf{z} , and the second term quantifies how much information \mathbf{x}_i provides about \mathbf{z} *in addition to* \mathbf{x}_ϕ . A feature \mathbf{x}_i will be penalized by the second term, if it is informative about \mathbf{z} but not about \mathbf{x}_ϕ . All quantities in the KL divergences above can be computed analytically thanks to the Gaussian approximations. The expectations in Eqn. 3 can be approximated by Monte Carlo, by averaging over samples $\mathbf{x}_\phi, \mathbf{x}_i \sim p(\mathbf{x}_\phi, \mathbf{x}_i | \mathbf{x}_O)$ that can be shared between the two terms in Eqn. 3. The number of samples is denoted as M .

Methodology

In this section, we first introduce our improvements on the model and sampling scheme of the EDDI framework, and then elaborate on how to accelerate computations in the case of disease diagnosis. A summary of our FIT framework is presented at the end.

Model

During active variable selection, the inference network of the VAE should be capable to handle arbitrary partial observations of feature variables. The EDDI framework (Ma et al. 2019) proposed a permutation invariant set function, given by

$$\mathbf{c}(\mathbf{x}_O) := g(h(\mathbf{s}_1), h(\mathbf{s}_2), \dots, h(\mathbf{s}_{|O|})), \quad (4)$$

where $|O|$ is the number of observed variables and \mathbf{s}_i is obtained from the product of the feature value x_i and an embedding vector \mathbf{e}_i describing the i -th feature. The value of

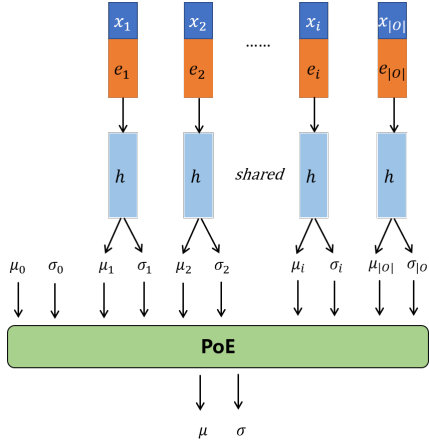


Figure 2: Overview of Products-of-Experts (PoE) encoder.

the embedding vector is optimized during training together with the recognition network. $h(\cdot)$ is a neural network and $g(\cdot)$ is summation or max-pooling operation.

Product of Experts (PoE) Encoder The Multimodal Variational Autoencoder (MVAE) was proposed by Wu and Goodman (2018) to capture a joint distribution across data modalities and flexibly support missing multimodal data. The MVAE assumes conditional independence among data modalities and uses a **PoE encoder** to approximate the joint posterior for the latent variables. The PoE approximate posterior, including a prior expert $p(\mathbf{z})$, is given by

$$q(\mathbf{z}|\mathbf{x}_1, \dots, \mathbf{x}_{|O|}) \propto p(\mathbf{z}) \prod_{i=1}^{|O|} q(\mathbf{z}|\mathbf{x}_i), \quad (5)$$

where $q(\mathbf{z}|\mathbf{x}_i)$ is an inference network representing the expert associated with the i -th observed variable \mathbf{x}_i .

In our implementation of the PoE encoder, we first, construct \mathbf{s}_i by concatenation: $\mathbf{s}_i = [\mathbf{x}_i, \mathbf{e}_i]$, which is widely used in the computer vision domain (Qi et al. 2017). Then we use an MLP with 4 hidden layers as $h(\cdot)$ to map the input \mathbf{s}_i to a factorized Gaussian distribution in latent space with mean vector μ_i and marginal standard deviation σ_i . Because a product of Gaussian experts is itself Gaussian (Cao and Fleet 2014), when $p(\mathbf{z})$ and $q(\mathbf{z}|\mathbf{x}_i)$ are Gaussian, we can compute the mean and covariance parameters for the distribution in Eqn. 5 easily:

$$\mu = (\sum_i \mu_i \mathbf{T}_i) (\sum_i \mathbf{V}_i^{-1})^{-1}, \mathbf{V} = (\sum_i \mathbf{V}_i^{-1})^{-1}, \quad (6)$$

where μ and \mathbf{V} are the mean vector and covariance matrix, respectively. The structure of our PoE encoder is illustrated in Figure 2. The decoder, $p(\mathbf{x}|\mathbf{z})$, is given by a product of Bernoulli distributions whose probabilities are specified by a 4-layer MLP that receives input \mathbf{z} .

Given a dataset with no missing variables, if we trained the PoE encoder on all the available data, its performance would then be poor when the input presents missing entries since the PoE encoder never dealt with such situation

Algorithm 1 Overview of FIT framework.

Require: Training dataset \mathbf{X} ; Test dataset \mathbf{X}^* with no observations; Indices ϕ of target variables(diseases).

1: **Train VAE with PoE encoder and classifier** $C(\cdot)$ on \mathbf{X}

2: **Actively acquire symptom** \mathbf{x}_i to estimate \mathbf{x}_ϕ^* by $C(\cdot)$

for each test point:

for each test point **do**

$\mathbf{x}_O \leftarrow \{\mathbf{x}_y\}$ (initial symptom)

$S \leftarrow S_y$

repeat

for every symptom \mathbf{x}_i in S **do**

$m \leftarrow 0$

repeat

 // Two-step sampling

$\hat{\mathbf{z}} \sim q(\mathbf{z}|\mathbf{x}_O)$

$\hat{\mathbf{x}}_i \sim \hat{p}(\mathbf{x}_i|\mathbf{z})$

$\hat{R}_{i,m} \leftarrow 0$

if $\hat{\mathbf{x}}_i$ is positive **then**

$\hat{\mathbf{x}}_\phi \sim C(\hat{\mathbf{x}}_i, \mathbf{x}_O)$

$\hat{R}_{i,m} \leftarrow$ Eqn. 3

end if

$m \leftarrow m + 1$

until $m = M$

$\hat{R}_i \leftarrow \frac{\sum_m \hat{R}_{i,m}}{M}$ // Positive attention reward

end for

 choose symptom \mathbf{x}_t with maximum reward \hat{R}_t

$\mathbf{x}_O \leftarrow \mathbf{x}_i \cup \mathbf{x}_O$

if \mathbf{x}_i is positive **then**

$S \leftarrow S_i \cap S$ // Filtering irrelevant symptoms

end if

until reaching maximum steps T or $\hat{R}_t < \epsilon$

end for

at training time. To address this, we follow Wu and Goodman (2018) and drop a random fraction of the fully observed variables for each data point during training. Later, we report experiments on active variable selection that show that this encoder out-performs the original EDDI encoder described in Eqn. 4.

Note that we may want to make predictions for possible diseases at any step of the feature collection process. This is something that RL methods are sub-optimal at since they use a classifier that is trained to make predictions once the RL agent stops collecting data and not at any stage of the data collection process. FIT does not have this problem. In particular, in FIT, we denote by $C(\cdot)$ the function returning the disease prediction probabilities $p(\mathbf{x}_\phi|\mathbf{x}_i, \mathbf{x}_O)$. We use an MLP classifier with 4 hidden layers as the $C(\cdot)$. In contrast to the training of VAE, we train $C(\cdot)$ on the complete data. Therefore, to make predictions, the missing variables of input are imputed by zero when fed into $C(\cdot)$. Our experiments show that the imputation would not affect the accuracy of disease-prediction.

Two-step Sampling Strategy To estimate the information reward, we approximate expectations by Monte Carlo. In

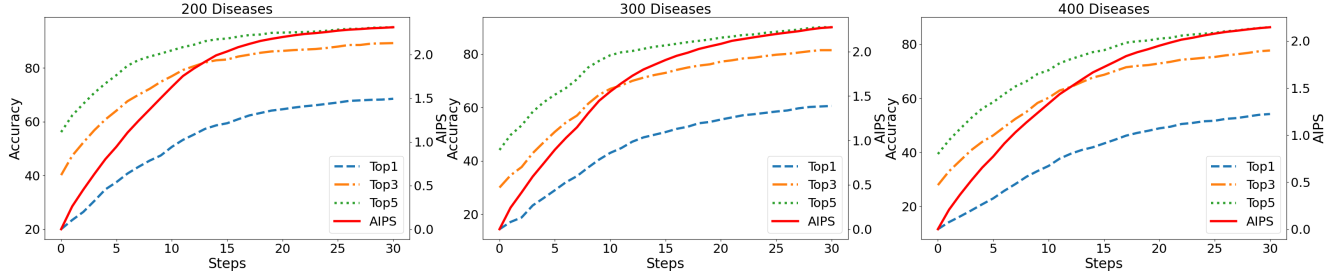


Figure 3: Evolution of accuracy and AIPS as the number of inquiry steps increases in FIT framework. AIPS stands for "Average Number of Inquired Positive Symptoms".

particular, we average over samples $\hat{\mathbf{x}}_\phi, \hat{\mathbf{x}}_i \sim p(\mathbf{x}_\phi, \mathbf{x}_i | \mathbf{x}_O)$. This can be implemented by first sampling $\hat{\mathbf{z}} \sim q(\mathbf{z} | \mathbf{x}_i)$, and then $\hat{\mathbf{x}}_\phi, \hat{\mathbf{x}}_i \sim \hat{p}(\mathbf{x}_\phi, \mathbf{x}_i | \mathbf{z})$, where $\hat{p}(\mathbf{x}_\phi, \mathbf{x}_i | \mathbf{z})$ is the decoder network in the EDDI VAE. However, we propose a better sampling method for FIT, which samples $\hat{\mathbf{x}}_i$ and $\hat{\mathbf{x}}_\phi$ in two steps. Note that

$$p(\mathbf{x}_\phi, \mathbf{x}_i | \mathbf{x}_O) = p(\mathbf{x}_\phi | \mathbf{x}_i, \mathbf{x}_O) \cdot p(\mathbf{x}_i | \mathbf{x}_O). \quad (7)$$

Therefore, we propose to sample $\hat{\mathbf{x}}_i$ from the VAE by sampling $\hat{\mathbf{z}} \sim q(\mathbf{z} | \mathbf{x}_O)$, and then $\hat{\mathbf{x}}_i \sim \hat{p}(\mathbf{x}_i | \mathbf{z})$. Next we sample $\hat{\mathbf{x}}_\phi$ from $C(\hat{\mathbf{x}}_i, \mathbf{x}_O)$. In this way we are actually using two networks (the VAE decoder and $C(\cdot)$) to decompose the approximation of the joint posterior. By combining the generative model and the classification model we can help improve the performance of entire framework. Our experiments (Table 2) show that this two-step sampling process provides better results than the original approach.

Speedup

The computational cost of the EDDI framework (Ma et al. 2019) is $O(T \cdot N \cdot M)$, where T is the number of maximum inquiry steps, N is the number of total features, and M is the number of samples used in the Monte Carlo approximation. In practice, this is too high for an online service. In what follows, we show how we can reduce the cost by a large amount by taking advantage of feature sparsity.

Filtering Irrelevant Symptoms At each step, the EDDI framework chooses variable \mathbf{x}_i from $U \setminus \phi$ to maximize the information reward. Under the setting of inquiry for symptoms, we can filter irrelevant symptoms to reduce the number of variables that need to be queried. For example, if a patient comes to visit a doctor with a broken leg, the first question from the doctor shall not be "Do you cough a lot?".

For every symptom i , we calculate the set S_i of additional symptoms which may appear together with symptom i in one patient with high probability, according to training data statistics. More specifically, a symptom $j \in S_i$ if $p_{data}(x_j = 1 | x_i = 1)$ is larger than a given threshold p . We simply set p to 0 in experiments. The set of candidate symptoms is initialized to S_i when symptom i is present at the beginning of the inquiry. Every time the framework selects an additional positive symptom j , we update the set of candidate symptoms to be the intersection of the current set and S_j (see Algorithm 1).

Attention on Positive Symptoms The number of symptoms that a patient of a certain disease suffers from is much smaller than the number of possible symptoms for the disease. With such a sparse feature space, the inquiry process should acquire positive symptoms, otherwise there is not enough evidence for the diagnosis component to perform accurate predictions (Peng et al. 2018). Motivated by this, we encourage FIT to discover positive symptoms, which drastically reduces computational cost without degrading prediction accuracy.

We implement the previous approach when evaluating the information reward of symptom i . For this, we first obtain M samples $\hat{\mathbf{x}}_i$ from $\mathbf{x}_i \sim p(\mathbf{x}_i | \mathbf{x}_O)$. Then, for each $\hat{\mathbf{x}}_i$ that is positive, we sample a corresponding $\hat{\mathbf{x}}_\phi$, and evaluate $\hat{R}(i, \mathbf{x}_O)$ according to Eqn. 3 with expectations replaced by evaluations on $\hat{\mathbf{x}}_i$ and $\hat{\mathbf{x}}_\phi$. By contrast, $\hat{R}(i, \mathbf{x}_O)$ is zero for each negative $\hat{\mathbf{x}}_i$. The information reward is then

$$\hat{R}_i = \frac{\sum_{m: \hat{\mathbf{x}}_{i,m}=1} \hat{R}_{i,m}}{M} \quad (8)$$

and, unlike in EDDI, we do not average across all samples.

The two previous techniques result in a speed-up of 1000x experimentally.

Overview of the FIT Framework

Algorithm 1 illustrates how the FIT framework is implemented in practice by combining the previous techniques, where ϵ is a small threshold that determines when to stop and that we set to 10^{-4} .

Related Work

Bayesian Inference and Tree-Based Methods There is a significant amount of previous work dealing with self-diagnosing. One large family of models applies Bayesian inference and tree-based methods (Kononenko 1993, 2001; Xu et al. 2013; Kohavi 1996), which use entropy functions to pick symptoms on the basis of the theory of information gain. For instance, Nan, Wang, and Saligrama (2015, 2016) and Zakim et al. (2008) proposed to address the cost of feature acquisition by using decision tree and random forest methods. In addition to this, Hayashi (1991) attempted to extract rule-based representations from medical data and human knowledge with the goal of performing disease diagnosis. Since the global maximization of the information gain

#Diseases	REFUEL (Peng et al. 2018)					FIT				
	Top1	Top3	Top5	AIPS	#Steps	Top1	Top3	Top5	AIPS	#Steps
200	54.84	73.66	79.68	1.40	8.01	56.21 ± 0.18	81.66 ± 0.13	89.67 ± 0.13	2.00 ± 0.00	13.67 ± 0.00
300	47.49	65.08	71.17	1.37	8.09	47.86 ± 0.22	73.51 ± 0.18	83.68 ± 0.17	1.83 ± 0.00	13.83 ± 0.00
400	43.83	60.76	67.09	1.31	8.35	44.50 ± 0.17	68.78 ± 0.11	79.16 ± 0.15	1.78 ± 0.00	14.86 ± 0.00

Table 1: Performance of REFUEL (Peng et al. 2018) and FIT framework on synthetic SymCAT dataset. The results of FIT framework are shown in percentage with a 95% confidence interval.

#Diseases	Method	Top1	Top3	Top5	AIPS	#Steps
300	EDDI	33.6 ± 0.6	56.9 ± 0.9	71.3 ± 0.8	1.06 ± 0.01	9.25 ± 0.03
	EDDI + two-step sampling	34.6 ± 0.4	57.8 ± 0.6	72.5 ± 0.8	1.13 ± 0.02	9.52 ± 0.04
	EDDI + PoE	47.7 ± 0.6	71.5 ± 0.4	82.6 ± 0.4	1.88 ± 0.01	13.85 ± 0.01
	EDDI + two-step sampling + PoE	48.3 ± 0.4	72.0 ± 0.4	82.7 ± 0.5	1.91 ± 0.01	13.85 ± 0.01

Table 2: Ablation study of the PoE encoder and two-step sampling scheme, on the SymCat dataset. The results are shown in percentage with a 95% confidence interval.

is intractable, these methods often use greedy algorithms or approximation that result in low predictive accuracy.

RL Based Method Recently Janisch, Pevný, and Lisý (2019) show that reinforcement learning (RL) methods outperform tree-based methods in the task of sequential feature acquisition with a given cost function. In particular, Tang et al. (2016) first formulated the inquiry and diagnosis process as a Markov decision process and used RL to perform symptom checking based on a simulated environment and data. More recently, Peng et al. (2018); Kao, Tang, and Chang (2018) achieved competitive results even on medium search spaces. For instance, in (Peng et al. 2018), the top1 disease-prediction accuracy is 54.84%, 47.49% and 43.83% for cases with 200, 300 and 400 diseases respectively. Xia et al. (2020) use a Generative Adversarial Network (GAN) and policy gradients to implement an RL agent for automatic self-diagnosis. This method shows good performance on two public datasets with Top-1 accuracy equal to 73% and 76.9% for the cases of four and five different diseases, respectively. However, such a low number of diseases and low predictive accuracy are not acceptable in real-world applications.

Experiments

We evaluate FIT on two public synthetic datasets: SymCAT, a symptom-based disease database (AHEAD Research Inc 2017), and a rare disease database from the Human Phenotype Ontology¹. We also report results on two public medical dialogue datasets: Dxy (Xu et al. 2019) and MuZhi (Wei et al. 2018). Details regarding datasets and model structures are listed in the Appendix.

SymCAT

Owing to the difficulties in obtaining and sharing medical data under privacy laws (e.g., the Health Insurance Portability and Accountability Act; HIPAA), we follow Kao,

Tang, and Chang (2018) and work first with simulated medical data. For this, we use the SymCAT symptom-disease database (AHEAD Research Inc 2017), which consists of 801 diseases and 474 symptoms in total. For each disease in SymCAT, you have information about its symptoms including the symptom marginal probabilities. The simulation process first samples a disease and its related symptoms from the set of all diseases. Then, symptoms are generated by performing a Bernoulli trial on each extracted symptom according to its corresponding probability. For instance, if the disease "abscess of nose" is first sampled, and the probabilities of "cough" and "fever" under "abscess of nose" are 73% and 62% respectively, we obtain one data instance by sampling Bernoulli random variables according to these probabilities.

As in the experiments by Peng et al. (2018), we sample 10^6 , 10^5 and 10^4 data points for training, validation and testing. We use Adam (Kingma and Ba 2014) as optimizer. The initial learning rate is 10^{-4} and the batch size is 128.

To evaluate the performance of FIT, we follow Peng et al. (2018) and form three different disease diagnosis tasks, which contain respectively 200, 300 and 400 diseases to discriminate among. The number of possible symptoms is more than 300 while the average number of positive symptoms per patient is about 3. More properties of the dataset are listed in Table ?? in the Appendix. Typically, it is very hard to identify positive symptoms. Hence, besides predictive accuracy, we also report *the average number of inquired positive symptoms*, which we abbreviate as AIPS. At the beginning of the inquiring process, one positive symptom is chosen uniformly at random among the positive symptoms for that patient in particular, as a patient self-report. Therefore, the maximum AIPS is about 2. The experiments shown below are implemented by applying the speedup techniques mentioned in the previous section.

Figure 3 shows how accuracy and AIPS change as the number of inquiry steps increases on 1000 simulated patients. M is selected to be 200. It can be found that, when the number of inquiry steps is less than 15, the four curves

¹<https://hpo.jax.org/app/>

#Diseases	FIT (without speedup)	FIT (with FIS)	FIT (with FIS and APS)
200	$4,815,368 \times 200$ (1.0)	$766,573 \times 200$ (6.3)	1,048,605 (918.4)
300	$5,168,341 \times 200$ (1.0)	$994,136 \times 200$ (5.2)	1,097,482 (941.9)
400	$5,634,915 \times 200$ (1.0)	$1,317,205 \times 200$ (4.3)	1,246,399 (904.2)

Table 3: Ablation study of the proposed speedup scheme on SymCat. "FIS" refers to "Filtering Irrelevant Symptoms" and "APS" is the abbreviation of "Attention on Positive Symptoms".

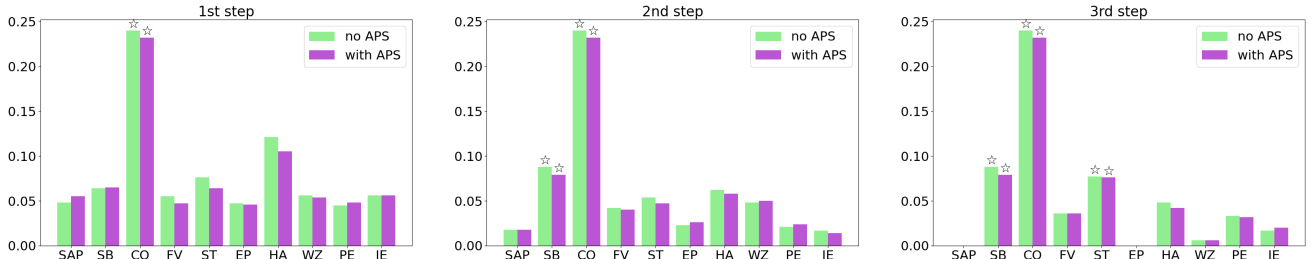


Figure 4: Distribution of information reward among several symptoms in first three inquiry steps. The symptoms with maximum reward are marked with star in every step. The initial symptom is "Nasal Congestion". "SAP" means "sharp abdominal pain". "SB" means "shortness of breath". "CO" means "cough". "FV" means "fever". "ST" means "sore throat". "EP" means "ear pain". "HA" means "headache". "WZ" means "wheezing". "PE" means "pain in eye". "IE" means "itchiness of eye".

in the figure all show the tendency of fast rising. And when the number of inquiry steps exceeds 15, the four curves still increase, but with less speed. When it gets to 30, all positive symptoms are almost inquired since AIPS reaches around 2. According to this, to perform as few steps as possible, we set the number of maximum inquiry steps to 14, 14 and 15 respectively for the tasks with 200, 300 and 400 diseases on 10,000 test patients, and report results in Table 1, where M was selected to be 200. We choose REFUEL (Peng et al. 2018), a SOTA reinforcement learning method on the synthetic SymCAT dataset, as a baseline. We can see that FIT outperforms REFUEL in every metric. In particular, the Top3 and Top5 accuracies are increased by at least 8 percent units. It is worth noting that the number of inquiry steps cannot be fixed, especially increased, in the RL-based method, which makes it unsuitable for some applications.

We study changes in accuracy and AIPS in FIT as the number of Monte Carlo samples M is increased. Figure ?? with these results can be found in the Appendix. The figure shows that it is reasonable to choose values of M that range from 200 to 400.

We performed an ablation study to investigate the effects of the PoE encoder and the two-step sampling strategy on the task with 300 diseases. We generated 1000 test patients and set M to 400. The number of maximum steps was fixed to 14. The encoder in the EDDI VAE (Ma et al. 2019) is chosen to follow the *Pointnet* (PN) setting (Qi et al. 2017). The results are presented in Table 2, which shows that the PoE encoder produces an improvement in accuracy of at least 10 percent units. By looking at the results for AIPS, it can be observed that the PoE encoder is affected to a small degree when the number of diseases increases. When looking at the number of steps, we can see that the EDDI framework tends

to stop early. At the same time, the PoE encoder seems to provide a narrower confidence interval, i.e. a more stable result. Finally, Table 2 shows that the two-step sampling strategy produces improvements in accuracy and AIPS in both tasks, especially in Top1 and AIPS, although in this case the gains are smaller.

Note that FIT could be easily extended to handle comorbidity, i.e. suffering from multiple diseases. In this case the different disease variables are considered to be independent. For the extension, all we need to change is to train a multi-label classifier instead of a multi-class one. Since we have not sought out appropriate data, we did not experiment with this possibility.

Speedup Ratio We performed another ablation study to show the acceleration given by the different elements within the proposed speedup scheme (filtering irrelevant symptoms and attention on positive symptoms). We generated 1000 simulated patients from SymCAT and set M as 200. The number of maximum inquiry steps is selected as 14. The results are presented in Table 3. Each entry in the table contains the number of samples used to calculate the information reward, which is the most time-demanding operation. The numbers in parenthesis are speed-up ratios as compared with the numbers in the first column. For instance, in the task with 200 diseases, without speedup, the EDDI framework checks over 4,815,368 symptoms totally, each requiring to draw 200 Monte Carlo samples to estimate the information reward. After filtering irrelevant symptoms, the sum of checked symptoms drops to 766,573 with 6.3 times less cost. If we only focus on the positive samples, the number of Monte Carlo samples that are used to calculate the reward for each candidate symptom is much lower than 200. The total number of samples is 1,048,605, which translates

#Diseases	REFUEL (Peng et al. 2018)				FIT			
	Top1	Top3	Top5	#Steps	Top1	Top3	Top5	#Steps
500	64.33	73.14	75.34	8.09	82.02	88.24	90.39	8.88
1000	40.08	62.67	67.42	14.19	63.33	72.67	76.33	13.71

Table 4: Performance of REFUEL (Peng et al. 2018) and FIT on synthetic rare disease dataset (HPO).

#Diseases	#Possible Symptoms	#Symptoms / Patient
500	1901	6.11
1000	3599	9.07

Table 5: Properties of dataset with rare diseases (HPO).

in 918.4 times less computational cost than the EDDI framework. This large reduction in cost allows each inquiry step to take less than one second on average.

We also performed a case study to show that Attention on Positive Symptoms makes little difference on the computed information reward values and on the actual symptoms queried by the framework. Figure 4 shows the partial distribution of information reward among different symptoms in the first three inquiry steps. The test data point is from the SymCAT task with 200 diseases and corresponds to a patient that suffers from *Common Cold*. The number of maximum steps was fixed to 14 and M was set to 200. A comparison for all inquiry steps is listed in Table ?? in the Appendix.

Rare Diseases

The Human Phenotype Ontology (HPO) provides a standardized vocabulary of phenotypic abnormalities for human disease. So far, HPO includes over 13,000 terms and 156,000 expert annotations to human hereditary diseases, obtained from multiple sources (the medical literature, Orphanet, DECIPIER, and OMIM). We downloaded diseases and related symptoms from the public rare disease dictionary, which includes 11,441 diseases and 13,032 annotated symptoms. We considered two different diagnosis tasks, each containing 500 and 1000 diseases to discriminate among. Our goal is to evaluate FIT in settings in which the number of symptoms is higher and closer to real-life applications: the number of symptoms is now 6 times larger than in SymCAT. More properties of the dataset are listed in Table 5. For these experiments, we generated 10,000 patients and set the maximum inquiry steps to 10 and 15 for the tasks with 500 and 1000 diseases, respectively. M was fixed to 100. While training REFUEL, the numbers of maximum inquiry steps are set to 14 and 18 respectively. We show results for FIT and REFUEL in Table 4. In this case, FIT outperforms REFUEL by a larger magnitude than before, with FIT’s accuracy being at least 10 percent units larger and the number of steps not increasing much when compared to REFUEL.

Two Real-life Dialogue Datasets

Wei et al. (2018) constructed the MuZhi Medical Dialogue dataset, which uses collected dialogue data from the pedi-

	MuZhi (Wei et al. 2018)	Dxy (Xu et al. 2019)
GAMP (Xia et al. 2020) FIT	73 73 \pm 1	76.9 77.3 \pm 0.7

Table 6: Accuracy of GAMP (Xia et al. 2020) and FIT framework on two public medical dialogue datasets. The results of FIT framework are shown in percentage with a 95% confidence interval.

atric department of a Chinese online healthcare website². MuZhi includes four diagnosed diseases: children’s bronchitis, children functional dyspepsia, infantile diarrhea infection and upper respiratory infection. There are 710 conversational data points, each representing a different patient, and 66 symptoms in total.

The Dxy Dialogue Medical dataset (Xu et al. 2019) contains data from a prevalent Chinese online healthcare website³, where people often inquire experts for professional medical advice. This dataset contains 527 dialogue data points, each one representing a different patient, five diagnosed diseases and 41 specific symptoms.

Table 6 shows results for GAMP (Xia et al. 2020), which uses GAN to implement an RL agent, and FIT on Dxy and MuZhi. FIT was implemented by setting M to 100 and the average inquiry steps to 16 and 11 for MuZhi and Dxy, respectively. These results show that FIT has competitive performance on these two real-life datasets, with slightly better accuracy when compared to GAMP.

Conclusion

We have proposed FIT, an information-based framework for fast and accurate disease self-diagnosis, which shows better performance than prior methods (Tang et al. 2016; Peng et al. 2018; Ma et al. 2019; Xia et al. 2020). We adopt a PoE Encoder to efficiently handle missing data and design a two-step sampling strategy to improve the quality of the generated samples. Both contributions result in higher disease diagnosis accuracy. We slightly modify previous calculations of the information reward to significantly speed up inference to a level that is practical in real-life settings while maintaining good disease-prediction accuracy. As the experiments show, our results in two simulated datasets, SymCAT and HPO, outperform existing baselines, and reveal that FIT can effectively deal with large search space problems at a

²<https://muzhi.baidu.com>

³<https://dxy.com/>

small cost of time. Furthermore, we evaluate FIT on two real-life datasets and achieve a competitive performance.

References

AHEAD Research Inc. 2017. SymCAT: Symptom-based, computer assisted triage. <http://www.symcat.com>.

Cao, Y.; and Fleet, D. J. 2014. Generalized product of experts for automatic and principled fusion of Gaussian process predictions. *arXiv preprint arXiv:1410.7827* .

Hayashi, Y. 1991. A neural expert system with automated extraction of fuzzy if-then rules and its application to medical diagnosis. In *Advances in neural information processing systems*, 578–584.

Janisch, J.; Pevný, T.; and Lisý, V. 2019. Classification with costly features using deep reinforcement learning. In *Proceedings of the AAAI Conference on Artificial Intelligence*, volume 33, 3959–3966.

Kao, H.-C.; Tang, K.-F.; and Chang, E. Y. 2018. Context-aware symptom checking for disease diagnosis using hierarchical reinforcement learning. In *Thirty-Second AAAI Conference on Artificial Intelligence*.

Kingma, D. P.; and Ba, J. 2014. Adam: A method for stochastic optimization. *arXiv preprint arXiv:1412.6980* .

Kingma, D. P.; and Welling, M. 2013. Auto-encoding variational bayes. *arXiv preprint arXiv:1312.6114* .

Kohavi, R. 1996. Scaling up the accuracy of naive-bayes classifiers: A decision-tree hybrid. In *Kdd*, volume 96, 202–207.

Kononenko, I. 1993. Inductive and Bayesian learning in medical diagnosis. *Applied Artificial Intelligence an International Journal* 7(4): 317–337.

Kononenko, I. 2001. Machine learning for medical diagnosis: history, state of the art and perspective. *Artificial Intelligence in medicine* 23(1): 89–109.

Ledley, R. S.; and Lusted, L. B. 1959. Reasoning foundations of medical diagnosis. *Science* 130(3366): 9–21.

Lewenberg, Y.; Bachrach, Y.; Paquet, U.; and Rosenschein, J. S. 2017. Knowing What to Ask: A Bayesian Active Learning Approach to the Surveying Problem. In *AAAI*, 1396–1402.

Ma, C.; Tschiatschek, S.; Palla, K.; Hernández-Lobato, J.; Nowozin, S.; and Zhang, C. 2019. EdDI: Efficient dynamic discovery of high-value information with partial VAE. In *36th International Conference on Machine Learning, ICML 2019*, volume 2019, 7483–7504.

Nan, F.; Wang, J.; and Saligrama, V. 2015. Feature-budgeted random forest. *arXiv preprint arXiv:1502.05925* .

Nan, F.; Wang, J.; and Saligrama, V. 2016. Pruning random forests for prediction on a budget. In *Advances in neural information processing systems*, 2334–2342.

Peng, Y.-S.; Tang, K.-F.; Lin, H.-T.; and Chang, E. 2018. Re-fuel: Exploring sparse features in deep reinforcement learning for fast disease diagnosis. In *Advances in neural information processing systems*, 7322–7331.

Qi, C. R.; Su, H.; Mo, K.; and Guibas, L. J. 2017. Pointnet: Deep learning on point sets for 3d classification and segmentation. In *Proceedings of the IEEE conference on computer vision and pattern recognition*, 652–660.

Semigran, H. L.; Linder, J. A.; Gidengil, C.; and Mehrotra, A. 2015. Evaluation of symptom checkers for self diagnosis and triage: audit study. *bmj* 351: h3480.

Shim, H.; Hwang, S. J.; and Yang, E. 2018. Joint active feature acquisition and classification with variable-size set encoding. In *Advances in neural information processing systems*, 1368–1378.

Tang, K.-F.; Kao, H.-C.; Chou, C.-N.; and Chang, E. Y. 2016. Inquire and diagnose: Neural symptom checking ensemble using deep reinforcement learning. In *NIPS Workshop on Deep Reinforcement Learning*.

Wei, Z.; Liu, Q.; Peng, B.; Tou, H.; Chen, T.; Huang, X.-J.; Wong, K.-F.; and Dai, X. 2018. Task-oriented dialogue system for automatic diagnosis. In *Proceedings of the 56th Annual Meeting of the Association for Computational Linguistics (Volume 2: Short Papers)*, 201–207.

Wu, M.; and Goodman, N. 2018. Multimodal generative models for scalable weakly-supervised learning. In *Advances in Neural Information Processing Systems*, 5575–5585.

Xia, Y.; Zhou, J.; Shi, Z.; Lu, C.; and Huang, H. 2020. Generative Adversarial Regularized Mutual Information Policy Gradient Framework for Automatic Diagnosis. In *Proceedings of the AAAI Conference on Artificial Intelligence*, volume 34, 1062–1069.

Xu, L.; Zhou, Q.; Gong, K.; Liang, X.; Tang, J.; and Lin, L. 2019. End-to-end knowledge-routed relational dialogue system for automatic diagnosis. In *Proceedings of the AAAI Conference on Artificial Intelligence*, volume 33, 7346–7353.

Xu, Z.; Kusner, M.; Weinberger, K.; and Chen, M. 2013. Cost-sensitive tree of classifiers. In *International conference on machine learning*, 133–141.

Zakim, D.; Braun, N.; Fritz, P.; and Alscher, M. D. 2008. Underutilization of information and knowledge in everyday medical practice: Evaluation of a computer-based solution. *BMC Medical Informatics and Decision Making* 8(1): 50.